Supplementary Material (ESI) for Chemical Communications


## - Electronic Supplementary Information -

# Selective co-aggregation of gold nanoparticles functionalised with complementary hydrogen bonding groups

*Coenraad R. van den Brom,[a,b] Petra Rudolf,[a] Thomas T.M. Palstra*[a] and Bart Hessen*[b]*

**Contents**



[a] *Zernike Institute for Advanced Materials, University of Groningen, Nijenborgh 4, 9747 AG Groningen, The Netherlands. Fax: +31 50 363 4441; Tel:+31 50 363 4419; E-mail t.t.m.palstra@rug.nl*
[b] *Stratingh Institute for Chemistry an d Chemical Engineering, University of Groningen, Nijenborgh 4, 9747 AG Groningen, The Netherlands. Fax: +31 50 363 4315; Tel: +31 50 363 4322; E-mail: b.hessen@rug.nl*

# 1. Determination of association constants of 1 and 2

The self-association behaviour of **1** and 6-(8-benzyl-sulfanyl-octyl)-[1,3,5]-triazine-2,4-diamine (**2a**) in $CDCl_3$ was studied. Here, **2a** was used rather than **2** because of the limited solubility of the latter in $CDCl_3$. Both **1** and **2a** show a concentration dependent shift for their amine-protons, indicative of homo-association.

*Experimental* All NMR-titration experiments were carried out with $CDCl_3$ freshly dried by filtration over activated (neutral) aluminium oxide powder. NMR-tubes were dried overnight at 150 °C before use. The titration series were prepared according to the guidelines of Wilcox[1]. The obtained chemical shifts were fitted as a function of the initial monomer concentration, using a fit function derived from an appropriate binding model that only includes dimerisation, assuming that the formation of complexes of a higher order than dimers is negligible:[2]

$$\delta_{obs} = \delta_H + \frac{x}{N} \cdot \frac{1+4A_0 - \sqrt{1+8A_0K_{ass}}}{8A_0K_{ass}} (\delta_{HH} - \delta_H)$$

Here, $\delta_{obs}$, $\delta_H$ and $\delta_{HH}$ are the observed chemical shift, and the shifts of a non-hydrogen-bonded and a hydrogen-bonded proton, respectively. $N$ is the number of equivalent protons in the molecule, whose shift is monitored, and $x$ is the number of H-bonded protons in the dimerised molecule. $A_0$ is the overall concentration of the species and $K_{ass}$ is the dimerisation constant. The complexation induced shift (CIS) is defined as CIS = $\delta_{obs}$, $\delta_H$. Fits were performed with a non-linear regression algorithm in Mathematica (Wolfram Research).

To study homo-association, stock solutions of 0.1M **1** or **2a** in $CDCl_3$ were prepared. Test solutions were made by diluting an amount of stock solution up to a total volume of 500 µl. Test solutions were prepared at concentrations ranging from 2 to 100 mM. All measurements were performed at 25 °C.

To study hetero-association, stock solutions of **1** and **2a** (8mM) in $CDCl_3$ were prepared by dissolution of 10.22 mg of **1** (37.5 µmol) and 13.82 mg of **2a** (37.5 µmol), respectively. Test solutions of 0.8 ml were prepared with a constant total concentration of ([**1**]+[**2a**]) = 8 mM. The fraction of **1** (defined as $f_1$=[**1**]/([**1**]+[**2**])) was varied from 0.2 to 0.8 in 11 equidistant steps. The amine chemical shift of thymine was monitored and used to compile a Job-plot, according to the formula[2] $F_{Job}=f_1(\delta_{obs} - \delta_{homo})$. The chemical shift in the absence of **2a**, $\delta_{homo}$ was calculated from its homo-dimerisation constant using the model and data presented above.

*Results* NMR titration curves for **1** and **2a** are shown in figure S1. For **1**, $K_{ass}$ = 4.7 $M^{-1}$ and CIS = 3.4 ppm; for **2a** $K_{ass}$ = 2.3 $M^{-1}$ and CIS = 5.1 ppm. These values are close to those obtained for 1-*N*-propylthymine (4.3 $M^{-1}$) and for 2,4-diamino-6-dodecyl-[1,3,5]triazine (2.2$M^{-1}$).[3] The Job-plot for **1**-**2a** association presented in figure S2 has a maximum at 0.5 indicative of the formation of the expected 1:1 complexes. The agreement of the H-bonding behaviour of the separate ligands with literature, makes it likely that the association constant of the hetero-complex also corresponds to the value of *ca.* 890 $M^{-1}$ reported for the dimerisation of the homologous complex of 6-dodecyl-[1,3,5]triazine-2,4-diamine and 1-*N*-propylthymine in literature.[3]

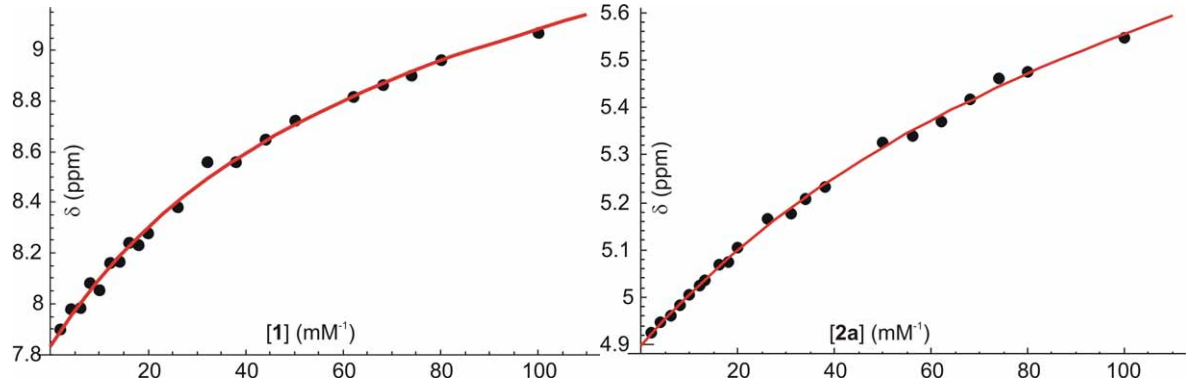


**Figure S1.** NMR titration curves of **1** (left) and **2a** (right). The measured values are represented by dots, the curves represent fits based on a dimerisation model.

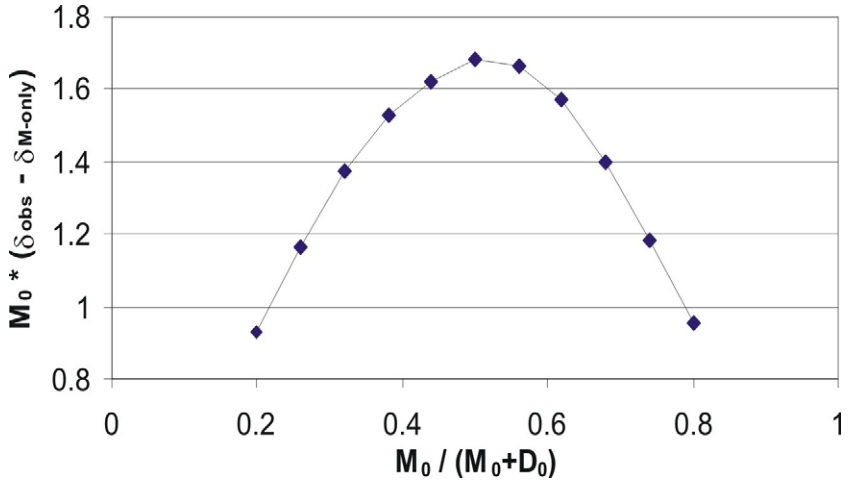


**Figure S2.** Job-plot of **1** and **2a**, at a 'total concentration' of $[\mathbf{1}]_0+[\mathbf{2}]_0$ = 8 mM.

## 2. Synthesis and characterisation of the cluster compound 4

$Au_{55}[P(C_6H_5)_3]_{12}Cl_6$ clusters were synthesised according to a method descibed in literature[4] and functionalised with either **2** *via* a ligand-exchange reactions. A fine powder was made of 12.7 mg of **2** (49 µmol) and was suspended ultrasonically in 50 ml $CH_2Cl_2$. To a Schlenk-flask containing 20 mg (1.4 µmol) of $Au_{55}[P(C_6H_5)_3]_{12}Cl_6$ 50 ml of benzene was added. The DTOT-suspension was then added to the dark-brown $Au_{55}$ solution via a septum. After stirring for 21 hours, a dark suspension in a colorless solution resulted. It was centrifuged at 4000 rpm for 30 min. and decanted. Then, the material was further purified by suspending ultrasonically in 50~ml acetonitrile, centrifuging and decanting three times and drying in vacuo. Yield: 16~mg.

*Transmission electron microscopy:* TEM investigations were carried out with a Philips CEM 120 transmission electron microscope, equipped with a $LaB_6$ filament. The microscope was operated at 120 kV. Images were acquired with a built-in Gatan 794 CCD-camera (1024×1024 pixels), controlled by Gatan Digital Micrograph v3.5 software. A TEM sample of **4** was investigated using an amorphous carbon support-film of several nanometers thickness on a 3 mm 400 µm mesh copper grid, on which. the cluster material was deposited from a dilute solution in DMSO, putting a droplet of about 0.05 ml on the film, rapidly followed by blotting off most liquid with filtration paper. A representative micrograph and corresponding cluster size distribution are displayed in figure S3. De size distribution was determined by digital image analysis using Matrox Inspector 2.1.

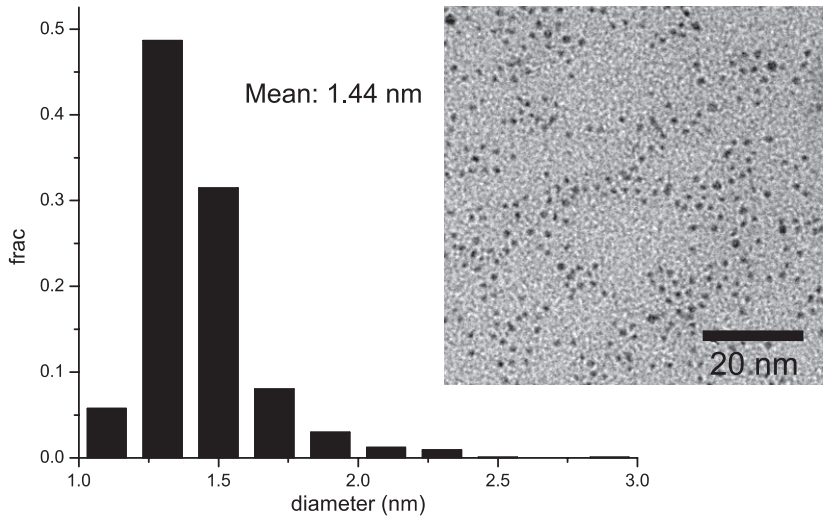


**Figure S3.** Transmission electron microscopy of $Au_{55}\boldsymbol{DTOT}_{15}[P(C_6H_5)_3]_8Cl_4$ (**4**)

*X-ray Photoelectron Spectroscopy:* An XPS sample of **4** was prepared by spreading a small amount of its powder on a piece of weighing paper and picking it up with a piece of conductive carbon tape (SPI Supplies) stuck on a stainless steel sampleholder. XPS measurements were performed using a SSX-100 (Surface Science Instruments, West Sussex, UK) photoelectron spectrometer with a monochromatic Al $K_\alpha$ X-ray source ($h\nu = 1486.6$ eV). The energy resolution was set to 1.5 eV to minimize data acquisition time and the photoelectron take-off angle (TOA) was 37°. All binding energies were referenced to the Au $4f_{7/2}$ core level at 83.8 eV.[5] The base pressure in the spectrometer was in the low $10^{-9}$ mbar range. Spectral analysis included a linear background subtraction and peak reconstruction using mixed Gaussian-Lorentzian functions on a Shirley background, in a least squares curve-fitting program (Winspec) developed in the Laboratoire Interdisciplinaire de Spectroscopie Electronique, Facultés Universitaires Notre-Dame de la Paix, Namur, Belgium. The photo-emission peak areas of each element, used to estimate the amount of each species on the surface, were normalized by the sensitivity factors of each element tabulated for the SSX-100 photoelectron spectrometer. XPS spectra and fits for the Au 4*f*, P 2*p*, N 1*s*, Cl 2*p* and P 2*p* regions of **4** are displayed in figure S4. Results of the stoichiometric analysis can be found in table ST1.

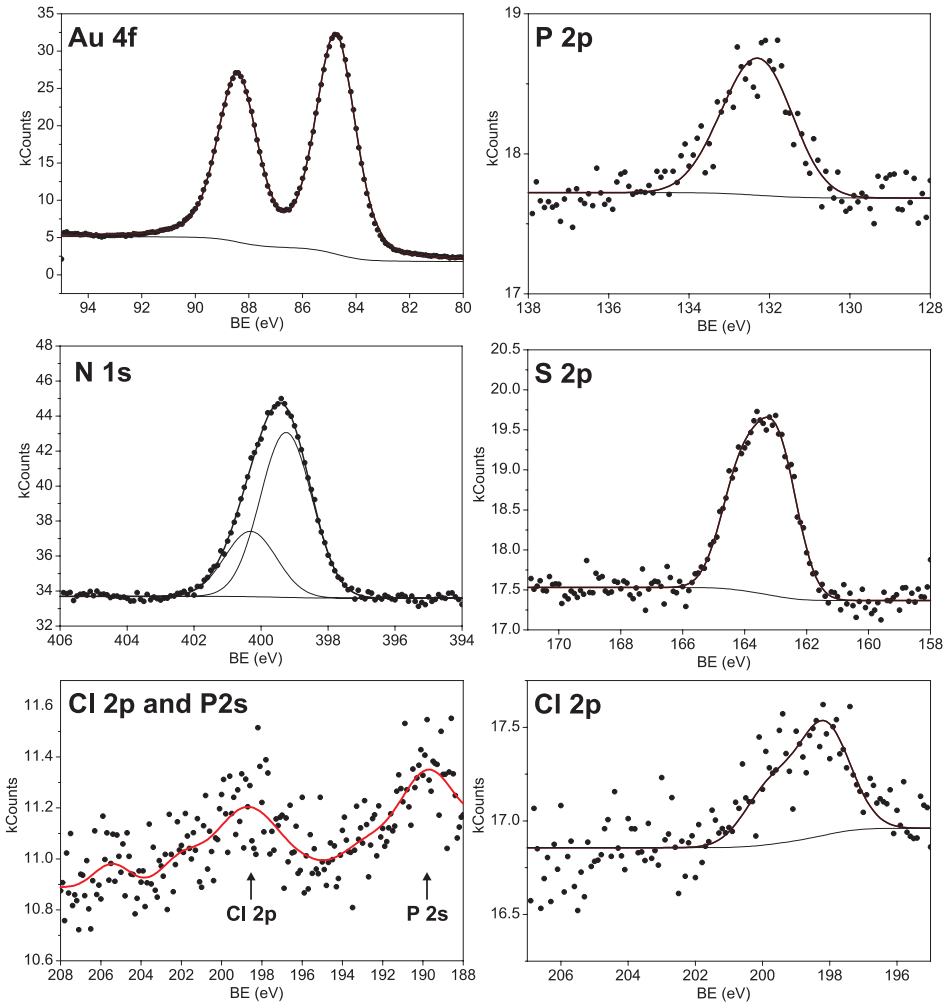


**Figure S4.** X-ray photoemission spectra of **4**. Measured data are represented by dots. Backgrounds and peak shapes obtained by modelling are shown as lines. In the *wide* Cl 2*p* spectrum a smoothed spectrum is included.

| Line | BE (eV) | FWHM (eV) | Stoich. | at-% |
|---|---|---|---|---|
| Au 4*f* | 84.6 | 1.8 | 55 [a] | 34 |
| S 2*p* | 162.8 | 1.8 | 15 ± 1 | 10 |
| N 1*s* (1) | 399.1 | 1.8[b] | 54 ± 3 | 34 |
| N 1*s* (2) | 400.1 | 1.8[b] | 21 | 14 |
| P 2*p* | 131.8 | 1.8[c] | 8 ± 1 | 5 |
| Cl 2*p* | 198.0 | 1.8[c] | 4 ± 1 | 2 |

[a]Reference value [b]Linked widths for these peaks [c]Fixed widths

**Table ST1.** Stoichiometric analysis of XPS data of $Au_{55}$–***MOT***

*Thermal analysis:* TGA measurements of **4** were performed with a TGA 7 (Perkin Elmer). 3–7 mg of material was heated in a platinum crucible at 10° C/min in a nitrogen atmosphere. Expected stoichiometry for **4**: $Au_{55}$***DTOT***$_{15}[P(C_6H_5)_3]_8Cl_4$, MW : 16888.88, expected mass loss: 36%, found: 30 %.

DSC analysis of **4** was performed with a DSC2920 (TA Instruments) by heating 3–4 mg of material in an aluminium pan at 10° C/min. The resulting calorigram is displayed in figure S5.

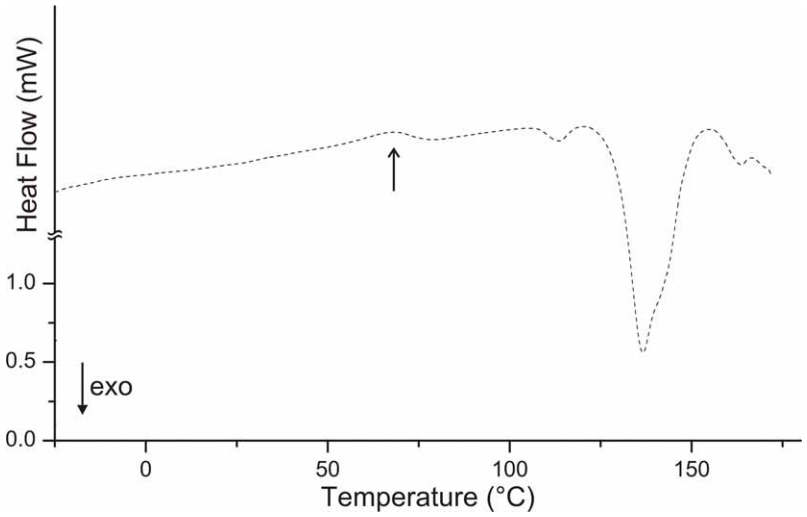


**Figure S5.** DSC analysis of **4**. The exothermal peak at 136.7°C (onset 129.4°C) corresponds to destruction of the cluster, which is observed at similar temperatures for other $Au_{55}$ clusters.[5] The weak endothermal peak at 66°C (onset 46°C) is ascribed to a "melting" phase transition of the ligand shell.[6]

## 3. *Hetero*-aggregates of 3 and 4

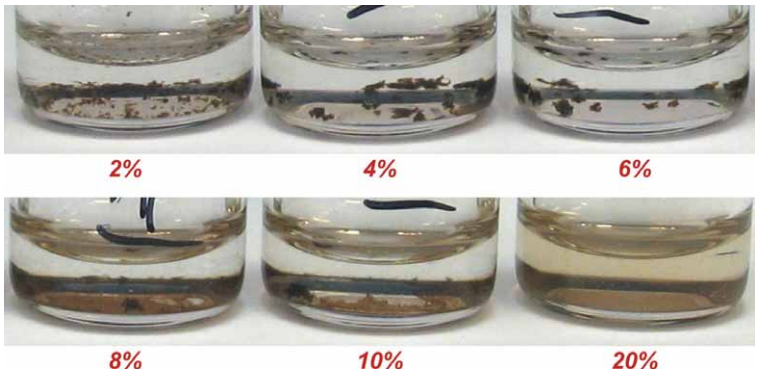


**Figure S6.** Photograph of vials (Ø *ca* 1.1 cm) containing aggregates formed in DMSO/dioxane mixtures when varying the DMSO concentrations from 2 to 20 % (*v*/*v*).

## 4. *Homo*-aggregation of 4

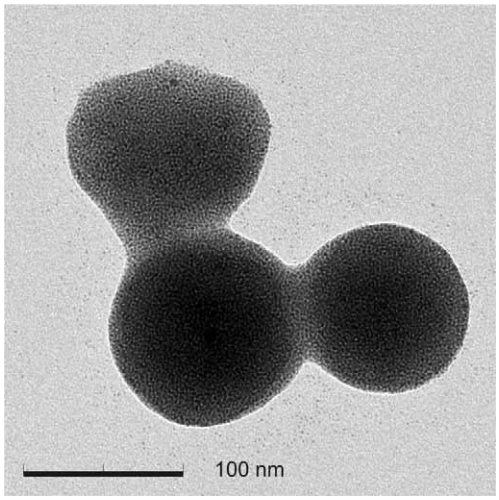


**Figure S7.** TEM micrograph of a typical example of the dense spherical aggregates of **4** formed from a mixture of 0.12 mg/ml **4** in DMSO/1,4-dioxane containing 2%(*v*/*v*) DMSO.

## 5. *Hetero*-aggregation of 3 and 4 in the presence of 1-*n*-hexyl-thymine

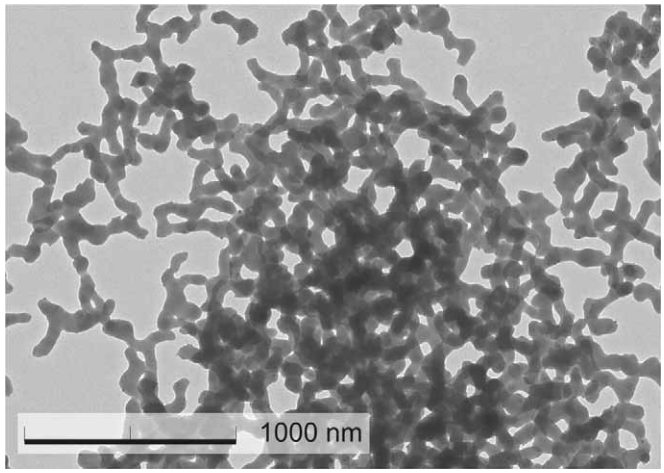


**Figure S8.** Morphology of *hetero*-aggregates of **3** and **4**, formed in the presence of $1.2 \cdot 10^3$ equivalents of 1-*n*-hexyl-thymine (**5**).

## 7. References

1. C. S. Wilcox, in *Frontiers in Supramolecular Organic Chemistry and Photochemistry*, ed. H.-J. Schneider, H. Dürr, VCH, Weinheim, 1991, Ch. 6, pp. 123-143.
2. K. A. Connors, *Binding Constants*, John Wiley & Sons, New York, 1987.
3. F. H. Beijer, R. P. Sijbesma, J. A. J. M. Vekemans, E. W. Meijer, H. Kooijman, and A. L. Spek, *J. Org. Chem.*, 1996, **61**, 6371–6380.
4. G. Schmid, *Inorg. Synth.*, 1990, **27**, 214–218.
5. R. C. Thiel, R. E. Benfield, R. Zanoni, H. H. A. Smit, and M. W. Dirken, *Struct. Bond.*, 1993, **81**, 1–39.
6. R. H. Terrill, T. A. Postlethwaite, C. Chen, C.-D. Poon, A. Terzis, A. Chen, J. E. Hutchison, M. R. Clark, G. Wignall, J. D. Londono, R. Superfine, M. Falvo, C. S. Johnson Jr., E. T. Samulski, and R. W. Murray, *J. Am. Chem. Soc.*, 1995, **117**, 12537–12548.